Lyapunov Analysis of Rigid Body Systems with Impacts and Friction via Sums-of-Squares

Michael Posa
Massachusetts Institute of Technology
77 Massachusetts Avenue
Cambridge, MA, USA
mposa@mit.edu

Mark Tobenkin
Massachusetts Institute of Technology
77 Massachusetts Avenue
Cambridge, MA, USA
mmt@mit.edu

Russ Tedrake
Massachusetts Institute of Technology
77 Massachusetts Avenue
Cambridge, MA, USA
russt@mit.edu

ABSTRACT

Many critical tasks in robotics, such as locomotion or manipulation, involve collisions between a rigid body and the environment or between multiple bodies. Sums-of-squares (SOS) based methods for numerical computation of Lyapunov certificates are a powerful tool for analyzing the stability of continuous nonlinear systems, which can play a powerful role in motion planning and control design. Here, we present a method for applying sums-of-squares verification to rigid bodies with Coulomb friction undergoing discontinuous, inelastic impact events. The proposed algorithm explicitly generates Lyapunov certificates for stability, positive invariance, and reachability over admissible (non-penetrating) states and contact forces. We leverage the complementarity formulation of contact, which naturally generates the semialgebraic constraints that define this admissible region. The approach is demonstrated on multiple robotics examples, including simple models of a walking robot and a perching aircraft.

Categories and Subject Descriptors

I.2.8 [**Computing Methodologies**]: Problem Solving, Control Methods, and Search—*control theory*; I.1.2 [**Computing Methodologies**]: Algorithms—*algebraic algorithms*; I.2.9 [**Computing Methodologies**]: Robotics—*kinematics and dynamics, manipulators*

Keywords

Lyapunov analysis and stability verification, rigid body dynamics with impacts and friction, sums-of-squares

1. INTRODUCTION

Many tasks in robotics require making and breaking contact with objects in the robot's environment. For highly dynamic tasks, such as walking [7, 35], and perching [8], this drives the need for control design techniques capable of handling impulsive dynamics and realistic friction models. Recent work has demonstrated that, for smooth nonlinear systems, techniques for stability verification can play a pivotal role in incremental motion planning and control design strategies, [30], and direct optimization over feedback laws [18]. Motivated by these developments, this paper presents a numerical approach for analyzing questions of stability, invariance, and reachability for rigid body systems subject to inelastic collisions and friction.

Our central observation is that the complementarity framework for modeling such systems (e.g. [4, 27, 12]) is compatible with recent advances in polynomial optimization, in particular sums-of-squares (SOS) optimization [23]. For a polynomial to be non-negative, it is sufficient that it be expressible as the sum of squares of polynomials. Optimizing over such polynomials can be formulated as a semidefinite program (SDP), a form of convex optimization. In the controls community, SOS has been widely applied, particularly in automating Lyapunov analysis of polynomial dynamical systems [10]. A major advantage of the complementarity framework over traditional approaches using hybrid automata is that non-smooth and impulsive dynamics can be expressed without suffering from the combinatorial explosion of "modes" resulting from distinct combinations of contacts. This approach also naturally encompasses instances of Zeno phenomena, which pose a challenge in some frameworks. Instead, the dynamics are described by conditions expressed jointly in the coordinates, velocities and feasible contact forces, the number of which grows linearly in the number of contact points.

This work demonstrates how Lyapunov analysis can be performed by testing sufficient semialgebraic conditions in these variables. We present algorithms based on testing these semialgebraic conditions using SOS optimization. Procedures for maximizing the size of regions of positive invariance or guaranteed regions of "safety" by solving a convex program (or a sequence of such programs) are provided. We apply the algorithms detailed here on multiple passive systems of interest to the robotics community.

1.1 Related Work

In this paper, we adopt the complementarity formulation for modeling rigid bodies with frictional impacts. This framework and its historical development are reviewed in [27] and a more comprehensive bibliography and discussion are provided in [4]. Notions of equilibria, stability, and extensions of Lyapunov analysis to such systems are presented

HSCC'13, April 8–11, 2013, Philadelphia, Pennsylvania, USA.

in [4] and [12] (see also the related article [13]). Section 2 will summarize the aspects of these works used in this paper.

An alternative formalism for modeling and control of non-smooth mechanical systems is that of hybrid automata [3]. Example applications of this framework to the control and analysis of hybrid mechanical systems can be found in [17], [26], and [21]. A number of numerical techniques have been presented for addressing verification, stability, and control design of general hybrid automata. These include methods based on approximate solutions of Hamilton-Jacobi equations, [31], and the construction of discrete abstractions [1]. SOS optimization has also been used to find polynomial barrier certificates, [24], as well as Lyapunov functions about equilibria, [22], and of transverse dynamics about hybrid limit cycles [19].

The fundamental difference between the approaches in [24], [22], and [19] and in this work stems from the choice of modeling framework. For a general rigid body with m possible contact points, 2^m different hybrid modes are possible, each with a distinct associated differential inclusion. By contrast, this work simultaneously reasons over the set of system trajectories and feasible contact force trajectories.

2. BACKGROUND

Here, we introduce a notion of solutions to discontinuous rigid body systems and describe the friction and impact laws used in this paper.

2.1 Measure Differential Inclusions

We consider systems whose state is given by a set of generalized coordinates $q \in \mathbb{R}^n$ and generalized velocities $v \in \mathbb{R}^n$ and we let $x = [q^T \; v^T]^T$. For mechanical systems, $q(t)$ will evolve continuously whereas $v(t)$ may have discontinuities due to impacts which present an obstacle to applying classical Lyapunov analysis.

Recently, a number of authors have provided extensions of Lyapunov analysis to discontinuous dynamics using the framework of *measure differential inclusions* (MDIs), see [12] Ch. 4 or [4] for more details. This framework addresses both the discontinuities and non-smoothness of the system evolution that arise from impacts and standard friction force laws. We provide a high-level overview of MDIs here, focused on autonomous Lagrangian mechanical systems.

A solution of a measure differential inclusion will be taken to be a pair of functions, $q(t)$ and $v(t)$, such that $q(t)$ is absolutely continuous and $v(t)$ is of locally bounded variation, allowing for countably many discontinuities. The left and right limits of $v(t)$, denoted $v^+(t)$ and $v^-(t)$, are guaranteed to exist and we require that solutions satisfy:

$$q(t) - q(t_0) = \int_{t_0}^{t} v(\tau) d\tau, \tag{1}$$

$$v^+(t) - v^-(t_0) = \int_{t_0}^{t} \dot{v}(\tau) d\tau + \int_{t_0}^{t} v^+(\tau) - v^-(\tau) d\eta(\tau). \tag{2}$$

Here $\dot{v}(t)$ is an integrable function and η is a sum of Dirac measures centered at times $\{t_k\}_{k=1}^{\infty}$, which model the continuous evolution of and jumps in the velocity respectively. By assumption, $v(t)$ has no singular part (see [12], Ch. 3). To describe the dynamics we must give rules for specifying legal values of $\dot{v}(t)$, the locations $\{t_k\}_{k=1}^{\infty}$, and the values of jumps $v^+(t_k) - v^-(t_k)$. Specific rules are given in the next section, but we briefly note the following: we require $\dot{v}(t) \in \mathfrak{F}(q(t), v(t))$ for almost all t, where $\mathfrak{F}(q, v)$ is a function which provides a *set* of possible values. This use of differential inclusions (i.e. set-valued laws) instead of equations is a standard approach for addressing Coulomb friction. Similarly, the value of jumps will be drawn from a set which generally depends on $q(t)$ and $v^-(t)$. The locations of impacts will be defined implicitly by the locations where $v^+(t)$ and $v^-(t)$ disagree. Finally, we take $v(t)$ to be undefined at points of discontinuity.

Our problems center around systems where solutions must lie in an *admissible set*, $\mathcal{A}$, defined by a finite family of functions $\phi_i : \mathbb{R}^n \to \mathbb{R}$:

$$\mathcal{A} = \{(q, v) \in \mathbb{R}^{2n} \mid \phi_i(q) \geq 0 \; \forall \; i \in \{1, \ldots, m\}\}. \tag{3}$$

Here the functions $\phi_i(\cdot)$ represent non-penetration constraints for the rigid body. We will focus on MDIs which are *consistent* (see [12], Ch. 4).

DEFINITION 1. *A measure differential inclusion is consistent if every solution defined for t_0 is defined for almost all $t \geq t_0$, all such solutions remain within $\mathcal{A}$, and for each $x_0 \in \mathcal{A}$ there exists at least one solution passing through x_0.*

An *equilibrium point* for such a system is defined as any point $x_0 \in \mathcal{A}$ such that such that $x(t) = x_0$ is a solution. In general we do not expect to have unique solutions from the systems covered by this work, particularly for models with dry friction ([4, 27]).

For systems governed by MDIs, natural extensions exist to the notions of stability and positive invariance ([12] Ch. 6). An equilibrium point $x_0 \in \mathcal{A}$ of a consistent MDI is *stable in the sense of Lyapunov* if, for each $\epsilon > 0$, there exists a $\delta > 0$ such that every solution $x(t)$ satisfying $|x_0 - x(t_0)| < \delta$ satisfies $|x_0 - x(t)| < \epsilon$ for almost all $t \geq t_0$. A set $B \subset \mathcal{A}$ is positively invariant if each solution $x(t)$ satisfying $x^-(t_0) \in B$ satisfies $x(t) \in B$ for almost all $t \geq t_0$.

In order to apply Lyapunov analysis to MDIs we make note of the following fact (see [12] Proposition 6.3): if $V : D \to \mathbb{R}$ is a continuously differentiable function on a compact set $D \subset \mathbb{R}^{2n}$, and $x(t)$ is of locally bounded variation, then $V(x(t))$ is of locally bounded variation and

$$V(x^+(t)) - V(x^-(t_0)) = \int_{t_0}^{t} \frac{\partial V}{\partial x} \dot{x}(\tau) d\tau + \int_{t_0}^{t} V(x^+(\tau)) - V(x^-(\tau)) d\eta(\tau), \tag{4}$$

where $\dot{x}(t) = [v(t)^T \; \dot{v}(t)^T]^T$, as in (1) and (2). For the remainder of this paper, when we write $\mathrm{d}V(x) \leq 0$ for certain $x \in A$ we mean that, for any solution satisfying $x^-(t) = x$, we have $\frac{\partial V}{\partial x} \dot{x}(t) \leq 0$ and $V(x^+(t)) - V(x^-(t)) \leq 0$.

2.2 Rigid Body Dynamics

Many robotic systems are appropriately modeled as a set of rigid links connected through some combination of joints. The continuous dynamics of these rigid body systems subject to frictional forces are well described by the manipulator equations

$$H(q)\dot{v} + C(q, v) = J(q)^T \lambda_N + J_f(q)^T \lambda_T, \tag{5}$$

where the dependence of q, v, λ_N, and λ_T on time has been suppressed for clarity. Here, $H(q)$ is the inertia matrix and $C(q, v)$ is the combined Coriolis and gravitational terms. In this paper, we primarily consider planar models, though the

extension to three dimensions is straightforward. For m potential contacts, the constraint forces are split into those normal to the contacts, $\lambda_N \in \mathbb{R}^m$, $\lambda_N \geq 0$, and the frictional forces tangential to the contact surface, $\lambda_T \in \mathbb{R}^m$. We will also write λ to be the stacked vector $\begin{bmatrix}\lambda_N^T & \lambda_T^T\end{bmatrix}^T$. The Jacobian matrices $J(q), J_f(q) \in \mathbb{R}^{m\times n}$ project the normal and frictional contact forces into joint coordinates. We will also refer to $J_i(q)$ and $J_{f,i}(q)$ as the ith row of the Jacobians associated with the particular contact forces $\lambda_{N,i}$ and $\lambda_{T,i}$.

We will focus on the dynamics of a planar rigid body contacting a fixed environment (such as the ground or a wall) at a finite number of contact points. Here, the velocity of the ith contact point has components $J_i v(t)$ and $J_{f,i} v(t)$ normal to and tangential to the contact surface. We use a simple Coulomb friction model to represent our contact forces:

$$J_{f,i}v(t) = 0 \Rightarrow |\lambda_{T,i}(t)| \leq \mu\lambda_{N,i}(t),$$
$$J_{f,i}v(t) \neq 0 \Rightarrow \lambda_{T,i}(t) = -\mathrm{sgn}(J_{f,i}v(t))\mu\lambda_{N,i}(t).$$

When the tangential velocity vanishes, $\lambda_{T,i}$ can take on any value within the friction cone. If the contact point is sliding, then $\lambda_{T,i}$ directly opposes the direction of slip.

2.3 Inelastic Collisions with Friction

Rigid body impacts are often modeled as instantaneous events where an impulse causes a discontinuity in the velocity. Impacts occur when there is contact, $\phi_i(q(t)) = 0$, and when the velocity normal to the contact would cause penetration, $J_i v^-(t) < 0$. As with the continuous case, we let $\Lambda_N, \Lambda_T \in \mathbb{R}^m$ be the normal and tangential impulses. Derived from the manipulator equations, the pre- and post-impact velocities for a collision at the ith contact point are related by $v^+(t) = v^-(t) + H^{-1}(J_i^T\Lambda_{N,i} + J_{f,i}^T\Lambda_{T,i})$. In the special case of frictionless inelastic collisions, we observe that the inelastic condition is $J_i v^+(t) = 0$ and so we can explicitly solve for the normal impulse and post-impact state:

$$\Lambda_{N,i} = -(J_i H^{-1} J_i^T)^{-1} J_i v^-(t), \tag{6}$$
$$v^+(t) = \left(I - H^{-1}J_i^T(J_iH^{-1}J_i^T)^{-1}J_i\right)v^-(t). \tag{7}$$

However, when considering Coulomb friction, we have no explicit formula. We provide a model for inelastic impacts into a single contact surface with friction. We additionally assume that simultaneous collisions, a well studied problem in both simulation and analysis[5], can be modeled as (potentially non-unique) sequences of single surface impacts.

To model frictional collisions, we adopt an impact law first proposed by Routh[25] that is described in detail in [34, 2]. Originally a graphical approach, this method constructs a path in impulse space that will fit naturally into our Lyapunov analysis. To briefly summarize Routh's technique for computing the net impulses and the post-impact state:

1. Monotonically increase the normal impulse $\Lambda_{N,i}$.
2. Increment the tangential impulse $\Lambda_{T,i}$ according to the friction law:
$$J_{f,i}\bar{v} = 0 \Rightarrow |\Lambda'_{T,i}| \leq \mu\Lambda'_{N,i},$$
$$J_{f,i}\bar{v} \neq 0 \Rightarrow \Lambda'_{T,i} = -\mathrm{sgn}(J_{f,i}\bar{v})\mu\Lambda'_{N,i},$$
where $\bar{v} = v^-(t) + H^{-1}(J_i^T\Lambda_{N,i} + J_{f,i}^T\Lambda_{T,i})$.
3. Terminate when the normal contact velocity vanishes, $J_i\bar{v} = 0$, and take $v^+(t) = \bar{v}$.

This method amounts to following a piecewise linear path in the impulse space where the slopes of the impulses are $\Lambda'_{N,i}$ and $\Lambda'_{T,i}$. Along each linear section, these slopes must satisfy the Coulomb friction constraints. Solutions may transition from sliding to sticking and vice versa and the direction of slip may even reverse as a result of each impact.

3. CONDITIONS FOR STABILITY

The highly structured nature of rigid body dynamics and the complementarity formulation of contact allow us to construct semialgebraic conditions for stability in the sense of Lyapunov and positive invariance.

3.1 Lyapunov Conditions for MDIs

We begin by describing sufficient conditions for stability in the sense of Lyapunov and positive invariance stated in terms of Lyapunov functions. Say that a function $\alpha : [0,\infty) \to [0,\infty)$ belongs to class $\mathcal{K}$ if it is strictly increasing and $\alpha(0) = 0$. The following theorem is adapted from [12], Theorem 6.23, and stated without proof.

THEOREM 1. *Let x_0 be an equilibrium point for a consistent MDI and let $V : \mathbb{R}^{2n} \to \mathbb{R}$ be a continuously differentiable function. If there exists a neighborhood U of x_0 and a class $\mathcal{K}$ function α such that $x \in U \cap \mathcal{A}$ implies $\mathrm{d}V \leq 0$ and $V(x) \geq \alpha(\|x - x_0\|)$ then x_0 is stable in the sense of Lyapunov.*

For a candidate Lyapunov function $V(q, v)$, define the c-sublevel set

$$\Omega_c = \{(q, v) \in \mathbb{R}^{2n} \mid V(q, v) < c\}.$$

For a system whose solutions are continuous functions of time, $\mathrm{d}V \leq 0$ on $\Omega_c \cap \mathcal{A}$ would be sufficient to show that each connected component of $\Omega_c \cap \mathcal{A}$ is positively invariant. However, where $v(t)$ is discontinuous, the pre- and post-impact states may be in disjoint connected components. The following lemma provides stronger conditions which guarantee positive invariance of such a connected component. The proof can be found in the Appendix.

LEMMA 2. *Let $V : \mathbb{R}^{2n} \to \mathbb{R}$ be a continuously differentiable function, and $\mathcal{C}$ be a connected component of $\Omega_c \cap \mathcal{A}$ with $\mathrm{d}V \leq 0$ on $\mathcal{C}$. Then $\mathcal{C}$ is positively invariant if, for every solution $(q(t), v(t))$ with $(q(t), v^-(t)) \in \mathcal{C}$, there exists a path $\bar{v}(s)$ from $v^-(t)$ to $v^+(t)$ such that $V(q(t), \bar{v}(s))$ is a non-increasing function of s.*

Lemma 2 holds for general Lyapunov functions and systems where the unilateral constraints are defined by the generalized positions q. While we are generally interested in systems with friction, we briefly consider the special structure implied by rigid body dynamics and frictionless, inelastic collisions. The following lemma, whose proof is in the Appendix, shows that for such systems, and for V a convex function in v for each fixed q, the above sufficient condition for positive invariance is also necessary. In particular, no additional conservatism is added by requiring $\bar{v}$ to be the chord connecting $v^-(t)$ to $v^+(t)$.

LEMMA 3. *For a rigid body system undergoing frictionless, inelastic collisions, let $V : \mathbb{R}^{2n} \to \mathbb{R}$ be a continuously differentiable function, and $\mathcal{C}$ be a connected component of $\Omega_c \cap \mathcal{A}$ such that $\mathrm{d}V \leq 0$ on $\mathcal{C}$. If V is convex in v for each fixed q the following conditions are equivalent:*

(i) $\mathcal{C}$ is positively invariant.

(ii) For each solution $(q(t), v(t))$, when $(q(t), v^-(t)) \in \mathcal{C}$, $V(q(t), \bar{v}(s))$ is non-increasing along the path $\bar{v}(s) = sv^+(t) + (1-s)v^-(t)$ for $s \in [0,1]$

The proof for Lemma 3 fails for contacts with friction as a result of the piecewise linear resolution of collisions. Solutions which transition from slip to stick or where the direction of slip reverses may have intermediate points during the Routh solution which leave Ω_c. The frictionless assumption does, however, cover a class of interesting problems including collisions due to impacting hard joint limits.

3.2 Conditions For Complementarity Systems

We now focus on Lagrangian mechanical systems with impacts and friction described by complementarity conditions. This section contains sufficient conditions for demonstrating $\mathrm{d}V \leq 0$ and the additional constraint on jump discontinuities in the statement of Lemma 2. We partition the admissible set, $\mathcal{A}$, into $\mathcal{F}$ and $\mathcal{A} \setminus \mathcal{F}$, where $\mathcal{F} = \bigcap_{i=1}^{m} \mathcal{F}_i$ and

$$\mathcal{F}_i = \{(q,v) | \phi_i(q) > 0\} \cup \{(q,v) | \phi_i(q) = 0,\ J_i(q)v > 0\}.$$

Intuitively, $\mathcal{F}$ is the region where there is no contact or all contacts are being broken which forces the contact forces to vanish. On $\mathcal{F}$, we know that $\lambda = \Lambda = 0$ and so that $\mathrm{d}V \leq 0$ is equivalent to

$$\nabla V(q,v)^T \begin{bmatrix} v \\ -H(q)^{-1}C(q,v) \end{bmatrix} \leq 0. \tag{8}$$

On $\mathcal{A} \setminus \mathcal{F}$, there may be frictional forces and collisions. The condition on continuous state evolution is simply

$$\nabla V(q,v)^T \begin{bmatrix} v \\ \dot{v} \end{bmatrix} \leq 0, \tag{9}$$

where (5) gives an expression for $\dot{v}$. We now provide conditions on V and a path for each jump discontinuity such that the requirements of Lemma 2 are satisfied. Furthermore, this path ensures that the jump conditions for $\mathrm{d}V \leq 0$ are met. We explicitly construct this path between pre- and post-impact states. Recall that the Routh method of Section 2.3 constructs a piecewise linear path through the space of contact impulses. We take $\bar{v}(s)$ to be the velocities defined in step 2 of the Routh method, where s is the path parameter varying the impulses. As $\bar{v}$ depends linearly on the forces, we can find the derivative of $\bar{v}$ with respect to s, defined along each path segment:

$$\frac{d\bar{v}(s)}{ds} = H^{-1}(J_i(q)^T \Lambda'_{N,i} + J_{f,i}(q)^T \Lambda'_{T,i}),$$

where $\Lambda'_{N,i}$ and $\Lambda'_{T,i}$ satisfy the Coulomb friction conditions. To show V is non-increasing along the path, we require

$$\left.\frac{\partial V(q,v)}{\partial v}\right|_{(q,\bar{v}(s))} H^{-1}(J_i^T \Lambda'_{N,i} + J_{f,i}^T \Lambda'_{T,i}) \leq 0. \tag{10}$$

Since the Routh method for resolving impacts is memoryless, any point $(q, \bar{v}(s))$ is also a possible pre-impact state. So the set of all possible $(q, \bar{v}(s))$ is precisely equivalent to $\mathcal{A} \setminus \mathcal{F}$ and it is equivalent to enforce (10) for all $(q,v) \in \mathcal{A} \setminus \mathcal{F}$ instead of along potential paths. This constraint must hold for all i, so we construct a single condition that encompasses all contact points:

$$\frac{\partial V(q,v)}{\partial v} H(q)^{-1}(J(q)^T \Lambda'_N + J_f(q)^T \Lambda'_T) \leq 0. \tag{11}$$

Both (9) and (11) are defined in terms of permissible contact forces λ and slopes of the impulse path Λ' when resolving a collisions. Complementarity conditions can be used to describe the set of feasible contact normal forces [4, 27, 12]:

$$\phi_i(q), \lambda_{N,i} \geq 0, \tag{12}$$
$$\phi_i(q)\lambda_{N,i} = 0, \tag{13}$$
$$(J_i(q)v)\lambda_{N,i} \leq 0. \tag{14}$$

These constraints prohibit contact at a distance and ensure that the contact normal is a compressive and dissipative force. Note that (12-14) apply not only to the continuous force λ, but they also describe the set of feasible impulse slopes Λ'. Observing that the friction constraints on both are also identical, we write the additional set of constraints:

$$(J_{f,i}(q)v)\lambda_{T,i} \leq 0, \tag{15}$$
$$\mu^2\lambda_{N,i}^2 - \lambda_{T,i}^2 \geq 0, \tag{16}$$
$$(\mu^2\lambda_{N,i}^2 - \lambda_{T,i}^2)(J_{f,i}(q)v) = 0. \tag{17}$$

Here, we diverge from the standard linear complementarity description of Coulomb friction to avoid introducing additional slack variables. However, for any (q,v), this full set of conditions is exactly equivalent to our formulations of both frictional, inelastic collisions and Coulomb friction.

We now have three separate positivity conditions for stability. On $\mathcal{F}$ we have (8) and on $\mathcal{A} \setminus \mathcal{F}$ we have (9) and (11), with the contact forces and impulses subject to (12-17). However, since the conditions on λ and Λ' are identical, observe that (9) is equal to the sum of (8) and (11), so it is a redundant condition. Note that since all of these conditions are continuous and all points in $\mathcal{A} \setminus \mathcal{F}$ are in the closure of $\mathcal{F}$, (8) holding on $\mathcal{F}$ implies that it will hold on all of $\mathcal{A}$. This precise overlap between the constraints on the forces and impulses allows us to restrict our attention to the conditions on (q, v, λ) for the remainder of the paper.

3.3 Semialgebraic Representation

Rigid body dynamics and the manipulator equations offer a great deal of structure that we can exploit to make the problems of control and verification more amenable to algebraic methods. For many rigid body systems, especially those of interest in robotics, trigonometric substitutions can reduce the task of kinematics to an algebraic problem[33]. Concretely, for rotational joints, substituting c_i and s_i for $\cos(q_i)$ and $\sin(q_i)$ respectively, with the constraint that $s_i^2 + c_i^2 = 1$, will often result in polynomial kinematics in c_i and s_i. For simple contact surfaces, the various terms of the manipulator equations and constraints (H, C, B, J, J_f, and ϕ) are also polynomial in c_i, s_i, v and the remaining translational coordinates of q. Several methods can be used to accommodate the appearance of $H(q)^{-1}$ in the conditions of the previous section. First we note that by explicitly introducing an additional variable $\dot{v} \in \mathbb{R}^n$, the condition (5) is algebraic in $\dot{v}, v, \lambda$, the translational components of q and any introduced trigonometric variables. Alternatively, as $H(q)$ is positive definite and polynomial, its inverse is a rational function and we can find equivalent conditions by clearing the denominator. These facts imply that

semialgebraic conditions can be posed that are equivalent to those in Section 3.2.

4. APPROACH

For our systems of interest, the Lyapunov conditions in Section 3 amount to non-negativity constraints on polynomials over basic semialgebraic sets. This formulation is amenable to SOS based techniques, which provide certificates that a polynomial can be written as a sum of squares of polynomials, a clearly sufficient condition for non-negativity. Searching over polynomials which satisfy these sufficient conditions can be cast as an SDP, allowing for the application of modern convex optimization tools. For the examples in this paper we use the YALMIP[15, 16] and SPOT[20] toolboxes to generate programs for the semidefinite solver SeDuMi[29]. For a portion of our approach, we exploit bilinear alternation (related to the techniques of DK-iteration [14] and also referred to as coordinate-wise descent). We briefly review these concepts in the Appendix.

4.1 Global Verification

For some dynamic systems, we can verify the Lyapunov conditions over the entire admissible set. Define $\mathcal{D}$ to be the set of all (q, v, λ) that satisfy the complementarity conditions (12-17). Note that this also implies $(q, v) \in \mathcal{A}$. If $(0, 0)$ is an equilibrium of the system, we can then pose the global feasibility SOS program:

$$\begin{aligned} \text{find} \quad & V(q,v) && (18)\\ \text{subj. to} \quad & V(0,0) = 0, \\ & V(q,v) \geq \alpha(||q|| + ||v||) && \text{for } (q,v) \in \mathcal{A}, \\ & \nabla V^T \begin{bmatrix} v \\ \dot{v} \end{bmatrix} \leq 0 && \text{for } (q,v) \in \mathcal{A}, \\ & \frac{\partial V}{\partial v} H^{-1}(J^T \lambda_N + J_f^T \lambda_T) \leq 0 && \text{for } (q,v,\lambda) \in \mathcal{D}, \end{aligned}$$

with $\alpha(\cdot)$ is in class $\mathcal{K}$ (see Section 3.1). SOS allows us to search over a parameterized family of polynomial Lyapunov functions via SDP. By finding such a function, we verify that every sublevel set of V is positively invariant and that the origin is stable in the sense of Lyapunov. This certificate of a nested set of invariant regions is weaker than asymptotic stability but stronger than invariance of a single set.

4.2 Regional Verification

For many problems of interest, we would like to maximize the verifiable region about an equilibrium. Specifically, find a Lyapunov function that maximizes the volume of a connected component $\mathcal{C} \subseteq \Omega_1 \cap \mathcal{A}$, which is positively invariant and, for all $\rho \leq 1$, $\mathcal{C} \cap \Omega_\rho$ is also positively invariant. This leads to the following optimization problem:

$$\begin{aligned} \max_{V} \quad & \text{Volume}(\mathcal{C}) && (19)\\ \text{subj. to} \quad & V(0,0) = 0, \\ & V(q,v) \geq \alpha(||q|| + ||v||) && \text{for } (q,v) \in \mathcal{C}, \\ & \nabla V^T \begin{bmatrix} v \\ \dot{v} \end{bmatrix} \leq 0 && \text{for } (q,v) \in \mathcal{C}, \\ & \frac{\partial V}{\partial v} H^{-1}(J^T \lambda_N + J_f^T \lambda_T) \leq 0 && \text{for } (q,v,\lambda) \in \mathcal{D} \\ & && \text{and } (q,v) \in \mathcal{C}. \end{aligned}$$

As currently posed, this problem is not amenable to convex optimization techniques. It is difficult to directly measure the volume of $\mathcal{C}$ and, as $\mathcal{C}$ is only one connected component of $\Omega_1 \cap \mathcal{A}$, it is not naturally described as a semialgebraic set. We approximate these regions by finding polynomials $g_i(q, v)$ and $g_o(q, v)$ such that their one sublevel sets ($\mathcal{G}_i$ and $\mathcal{G}_0$ resp.) are inner and outer approximations of $\mathcal{C}$, i.e.

$$(\mathcal{G}_i \cap \mathcal{A}) \subseteq \mathcal{C} \subseteq (\mathcal{G}_o \cap \mathcal{A}). \tag{20}$$

By containing $\mathcal{C}$ within the semialgebraic set $\mathcal{G}_o$ and verifying the Lyapunov conditions on $\mathcal{G}_o$, we provide sufficient conditions on $\mathcal{C}$. The inner approximation $\mathcal{G}_i$ is used to estimate the volume of the verified region. In practice, we parameterize g_i and g_o as quadratic forms. For $g_i(q, v) = \begin{bmatrix} q^T & v^T \end{bmatrix} G_i \begin{bmatrix} q^T & v^T \end{bmatrix}^T$, we will use $-\text{Trace}(G_i)$ as a proxy for the volume of $\mathcal{C}$. Given this, we pose the problem:

$$\begin{aligned} \min_{V, G_i, G_o} \quad & \text{Trace}(G_i) && (21)\\ \text{subj. to} \quad & V(0,0) = 0, \quad G_i, G_o \succeq 0, \\ & V(q,v) \geq \alpha(||q|| + ||v||) && \text{for } (q,v) \in \mathcal{A} \cap \mathcal{G}_o, \\ & \nabla V^T \begin{bmatrix} v \\ \dot{v} \end{bmatrix} \leq 0 && \text{for } (q,v) \in \mathcal{A} \cap \mathcal{G}_o, \\ & \frac{\partial V}{\partial v} H^{-1}(J^T \lambda_N + J_f^T \lambda_T) \leq 0 && \text{for } (q,v,\lambda) \in \mathcal{D} \\ & && \text{and } (q,v), \in \mathcal{G}_o, \\ & V(q,v) \geq 1 && \text{for } (q,v) \in \mathcal{A} \\ & && \text{and } g_o(q,v) = 1, \\ & V(q,v) \leq 1 && \text{for } (q,v) \in \mathcal{A} \cap \mathcal{G}_i. \end{aligned}$$

This problem verifies the Lyapunov conditions on the outer approximation $\mathcal{G}_o$ and ensures the containment in (20). It is now posed in the familiar form of an optimization over polynomials that are positive on a basic semialgebraic set. As described in the Appendix, we use a bilinear alternation technique to solve this problem. One of the potentially difficult aspects of this alternation is that we must typically supply an initial feasible Lyapunov candidate. Previous sums-of-squares based methods have used local linearizations of the dynamics to find initial candidates [32, 30], but this approach fails when the dynamics are discontinuous. However, since the passive rigid body dynamics and inelastic collisions are energetically conservative, taking V to be the total energy provides a viable starting point for most mechanical systems. Solutions to (21) are guaranteed to be feasible Lyapunov functions to the original problem (19), although they will generally be suboptimal. This method, however, provides a tractable technique to synthesize useful regional certificates through contact discontinuities.

An alternate approach to bilinear alternations is to fix $\mathcal{G}_o$ and to fix the form of $\mathcal{G}_i$ to within a scalar factor and pose (21) as a feasibility problem. The optimal scaling of G_i can then be found by binary search. Though it only searches over a subset of the solutions to the first formulation, this SDP may be better conditioned numerically for some applications.

4.3 Reachability

The algorithm above for verifying stability and invariance can be easily adapted to address questions of dynamic reachability. For instance, we might wish to determine the largest set of initial conditions such that the infinite horizon reach-

able set does not intersect some unsafe semialgebraic set $\mathcal{U}$. We pose this problem in a manner similar (21), although here we do not require that V be positive definite:

$$\begin{aligned}
\min_{V,G_i,G_o} \quad & \text{Trace}(G_i) && (22)\\
\text{subj. to} \quad & G_i, G_o \succeq 0,\\
& \nabla V^T \begin{bmatrix} v \\ \dot{v} \end{bmatrix} \leq 0 && \text{for } (q,v) \in \mathcal{A} \cap \mathcal{G}_o,\\
& \frac{\partial V}{\partial v} H^{-1}(J^T \lambda_N + J_f^T \lambda_T) \leq 0 && \text{for } (q,v,\lambda) \in \mathcal{D}\\
& && \text{and } (q,v) \in \mathcal{G}_o,\\
& V(q,v) \geq 1 && \text{for } (q,v) \in \mathcal{A}\\
& && \text{and } g_o(q,v) = 1,\\
& V(q,v) \leq 1 && \text{for } (q,v) \in \mathcal{A} \cap \mathcal{G}_i,\\
& V(q,v) \geq 1 && \text{for } (q,v) \in \mathcal{A} \cap \mathcal{U}.
\end{aligned}$$

The optimization program in (22) verifies that $\mathcal{C}$ is positively invariant and that $\mathcal{C} \cap \mathcal{U} = \emptyset$, so no trajectory that originates in $\mathcal{C}$ can leave the safe region.

5. EXAMPLES

5.1 Bean Bag Toss

We first examine the simple problem of a bean bag, modeled as a planar point mass, colliding with the ground. This example serves to demonstrate the method on a system simple enough where the calculations can be easily verified by hand. With $q = \begin{bmatrix} x & z \end{bmatrix}^T$ and $v = \begin{bmatrix} \dot{x} & \dot{z} \end{bmatrix}^T$, we define $\phi(q) = z$ and the dynamics are given by

$$m\ddot{x} = \lambda_T, \quad m\ddot{z} = -mg + \lambda_N.$$

For this simple system, the dynamics are invariant under x so we consider the equilibrium set where the mass rests on the ground, $\{(x,z) \in \mathbb{R}^2 | z = 0\}$. Choosing our Lyapunov candidate function be equal to the total energy of the system, we will show stability in the sense of Lyapunov and invariance of a series of nested sets. That is, each sublevel set of energy is positively invariant. Substituting $V(q,v) = .5m\dot{x}^2 + .5m\dot{z}^2 + mgz$ and the dynamics into (18), we have the two conditions:

$$-\nabla V^T \begin{bmatrix} v \\ \dot{v} \end{bmatrix} = -mg\dot{z} + mg\dot{z} \geq 0 \text{ for } (q,v,\lambda) \in \mathcal{D}, \quad (23)$$

$$-\frac{\partial V}{\partial v} H(q)^{-1}(J(q)^T \lambda_N + J_f(q)^T \lambda_T) = -\dot{x}\lambda_T - \dot{z}\lambda_N \geq 0 \text{ for } (q,v,\lambda) \in \mathcal{D}. \quad (24)$$

The first condition is trivially true. Observing that $Jv = \dot{z}$ and $J_f v = \dot{x}$, we use S-procedure type multipliers to verify the second condition. Generating sums-of-squares multipliers $\sigma_i(q,v,\lambda)$ for the relevant unilateral constraints (14) and (15), replace (24) with

$$-\dot{x}\lambda_T - \dot{z}\lambda_N + \sigma_1 \dot{x}\lambda_T + \sigma_2 \dot{z}\lambda_N \text{ is SOS.} \quad (25)$$

Choosing $\sigma_1 = \sigma_2 = 1$, the equation above vanishes and is trivially non-negative. Thus, we have used our methods to demonstrate the rather obvious fact that every sublevel set of energy will be positively invariant.

Note that there also exists a quartic Lyapunov function that satisfies (18) but where we can additionally verify that $\dot{V} < -\alpha(z^2 + \dot{x}^2 + \dot{z}^2)$ for some class $\mathcal{K}$ function α. Combined with the condition that $\mathrm{d}V \leq 0$, this is sufficient to verify asymptotic stability of the equilibrium set, though we do not prove this here. In general, it is difficult to find such Lyapunov functions for discontinuous mechanical systems.

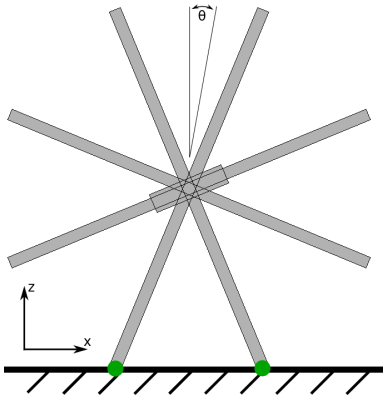

Figure 1: The rimless wheel shown in an equilibrium state, with two feet on the ground. Verified trajectories pass through four possible contact states (no contact, double-support, and both single-support phases).

Table 1: Rimless Wheel Parameters

mass	1 kg
moment of inertia	0.25 kgm^2
center to foot distance	1 m

5.2 Rimless Wheel

The rimless wheel model is a single rigid body composed of a number of equally-spaced spokes about a simple mass. This simple model has been used extensively as a proxy for a passive-dynamic walking robot[6]. Though previous works have primarily been interested in analyzing the limit-cycle behavior of the rimless wheel, here we focus on the stability of a single, static configuration of the system. We allow for frictional contacts between two of the spokes and the ground, highlighted in Fig. 1, and we consider the equilibrium set where both of these spokes rest on a flat ground. We differentiate between resting on these two particular spokes and any other equilibrium state. Trajectories of the rimless wheel that come to rest in the equilibrium set may undergo an infinite number of collisions rocking back and forth between the two feet, in an example of Zeno phenomena.

The planar floating base model of the rimless wheel has three degrees of freedom, $q = \begin{bmatrix} x & z & \theta \end{bmatrix}^T$ and $v = \begin{bmatrix} \dot{x} & \dot{z} & \dot{\theta} \end{bmatrix}^T$. With the trigonometric substitutions $s = \sin(\theta)$ and $c = \cos(\theta)$, the dynamics of the rimless wheel and the contact related elements $\phi_i(q)$, $J_i(q)$, and $J_{f,i}(q)$ are all polynomial functions of the redundant state variables $(x, z, s, c, \dot{x}, \dot{z}, \dot{\theta})$ and the contact forces $(\lambda_{N,i}, \lambda_{T,i})$. As with the point mass example, the dynamics are invariant under x and so the equilibrium set is defined as $\{(x,z,\theta) \in \mathbb{R}^3 | z = 0, \theta = 0\}$. The parameters of the rimless wheel model are given in Table 1.

Taking the total mechanical energy of the system as an initial candidate Lyapunov function, we search for a solution to (21) to find a nested set of invariant regions and verify

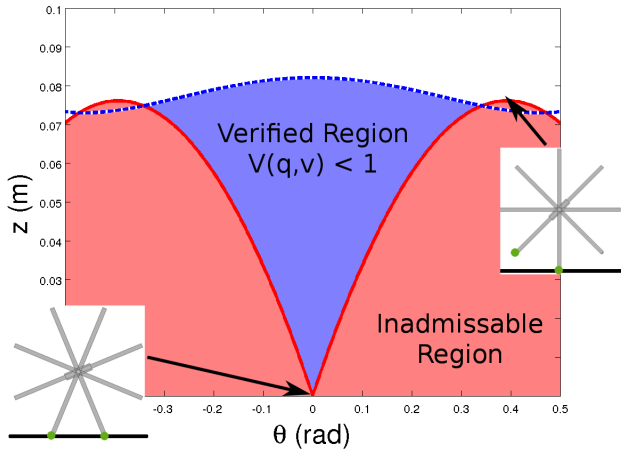

(a)

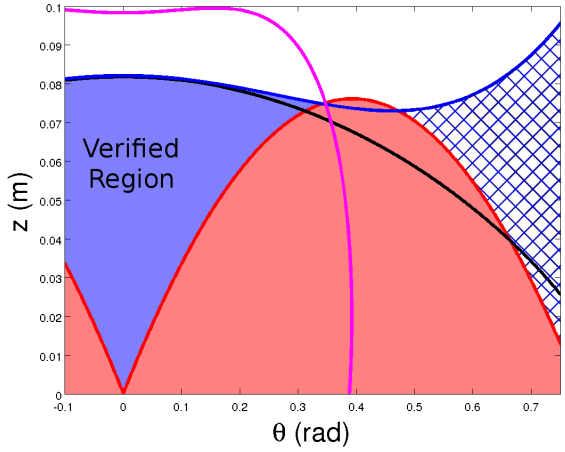

(b)

Figure 2: A slice of the rimless wheel state space is shown where all velocities are zero. (a) The red region below the solid line indicates the inadmissible set, where at least one of the contact points is penetrating the ground. For reference, two particular states are indicated: the stable equilibrium in double-support at the bottom and the unstable equilibrium in single-support on the upper right. The blue region below the dashed line is the connected component $\mathcal{C} \subseteq \Omega_1 \cap \mathcal{A}$ that contains the equilibrium (the verified region). (b) Two additional curves are shown. Under the black curve is $\mathcal{G}_i$, tight to $\Omega_1 \cap \mathcal{A}$, which we use to approximate the volume of the verified region. Under the magenta curve is $\mathcal{G}_o$, which must contain $\mathcal{C}$. $\mathcal{G}_o$ is parameterized as an ellipsoid in the redundant state variables, including s and $(1-c)$, which is why it is not convex when plotted against θ. The hatched region, while a subset of $\Omega_1 \cap \mathcal{A}$, is not connected to $\mathcal{C}$ and is unverified by our algorithm (and also outside the true invariant region).

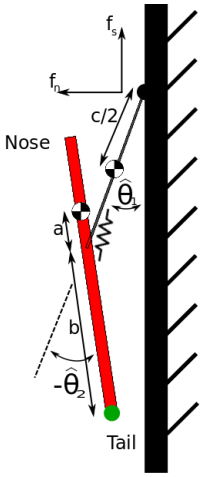

Figure 3: A simple model of a perching aircraft using two rigid links. The foot of the aircraft is pinned to the wall surface and there is a contact point at the tail that can collide with and slide along the wall. A torsional spring damper connects the main body of the aircraft to the foot.

stability in the sense of Lyapunov. When we parameterize V as a quartic polynomial, we verify a significant region of state space about the origin. A slice of this region is shown in Fig. 2(a) where the verified region is the connected component of $\Omega_1 \cap \mathcal{A}$ containing the origin. Fig. 2(b) illustrates the use of $\mathcal{G}_i$ and $\mathcal{G}_o$ to provide inner and outer bounds on $\mathcal{C}$.

It is interesting to note that if we parameterize V as a quadratic polynomial, the alternations quickly converge to verify a region that is nearly identical to the maximal sublevel set of energy that does not contain any additional equilibrium points. Additionally, we recover a scaled version of energy as our Lyapunov candidate. The quartic parameterization, however, verifies a larger region with a Lyapunov function significantly different from energy.

Note that the true region of attraction of this model is unbounded. For instance, for any x, z, take $q = \begin{bmatrix} x & z & 0 \end{bmatrix}^T$ and all velocities to be zero. A trajectory starting from any height will fall and then come to rest in the equilibrium set. By our parameterizations of $\mathcal{G}_i$ and $\mathcal{G}_o$, our regional approach is limited to ellipsoidal volumes and so will not recover the entire region of attraction. We do find a significant volume about the equilibrium set that would be relevant to planning or control applications.

5.3 Perching Glider

We lastly examine the problem of verifying a safe set of initial conditions for a glider perching against a wall, by adapting a model first presented in [8]. We consider the instant after the glider feet, which have adhesive microspines, have first impacted the wall and so we treat this contact as a pin joint. The glider is then modeled as a two-link body, with a spring damper connecting the bodies as shown in Fig. 3. We allow the tail of the glider to impact the surface of the wall and slide along it. The specific problem of verification was earlier addressed in [9], although the authors there used a model with a single joint and fixed the tail of the glider to slide along the wall, disallowing collisions. In

Table 2: Glider Properties

Body Mass	0.4 kg	Leg Length, c	0.15 m
Body Inertia	0.0164 kgm^2	Spring Const.	4.1e-3 Nm/°
Foot Mass	0.05 kg	Damper Const.	1.2e-4 Nms/°
Foot Inertia	0.001 kgm^2	Friction Coef. μ	0.3
Body CG, a	0.03 m	Nose Clearance	$\hat{\theta}_1 \geq 0$
Foot Dist., b	0.15 m	Force Limit	$f_s + f_n \geq 0$

this paper, we verify a significantly larger region than in our previous work, though a direct comparison is impossible since our model is higher dimension and uses Coulomb friction instead of viscous damping at the tail contact.

There are two relevant failure modes for the perching behavior of the glider, described in more detail in [9]. In one, the nose of the glider impacts the wall, which would be a potentially damaging event. In the other, the force limit of the feet microspines is exceeded and the glider falls from the wall. The force at the feet is a rational function of the state variables, and so the force limit can be easily expressed as a semialgebraic constraint. The full parameters of the glider are given in Table 2.

This is a two degree of freedom model, with $q = \begin{bmatrix}\hat{\theta}_1 & \hat{\theta}_2\end{bmatrix}^T$ and we again use a trigonometric substitution for both angles. We also change coordinates so that $(0, 0)$ is an equilibrium point with the tail resting against the wall, substituting $\theta_1 = \hat{\theta}_1 - .2604$ and $\theta_2 = \hat{\theta}_2 + .5207$. With the rimless wheel, $H(q)$ was a constant matrix and so $H^{-1}(q)$ was also constant. Here, $H(q)^{-1}$ is rational and so, for our dynamical constraints, we clear the denominator to ensure that our conditions are algebraic.

We search for a solution to (22), to maximize the set of initial conditions of trajectories that do not violate either constraint. Here, we let $\mathcal{G}_o$ be all of $\mathbb{R}^{2n}$ and define

$$\mathcal{G}_i(\rho) = \{(q, v) | 2(1 - c_1) + 2(1 - c_2) + 0.1||v||^2 < \rho\}.$$

We seek to maximize ρ through a binary search, observing that $2(1-c_i)$ well approximates θ_i^2 near $\theta_i = 0$. As with the rimless wheel, if we restrict our search to parameterizations of V of equal degree to energy, we recover the maximal sublevel set of energy that does not intersect either constraint boundary. If we expand our search to include all quartic polynomials, we find a Lyapunov function which verifies a visibly larger region. Two slices of this region are shown in Fig. 4(a) and 4(b). Our binary search terminates finding $\rho = 0.25$ and we can verify that an upper bound on the true optimal value is $\rho = 0.327$, since there $\mathcal{G}_i(\rho)$ intersects the constraint boundary. Of course, the true optimal value might be lower still since there is no claim that any $\mathcal{G}_i(\rho)$ is invariant. Here, we find a significant invariant region that usefully approximates the safe set of initial conditions.

6. CONCLUSIONS

Reliable planning and control through contact, as in locomotion and manipulation tasks, are critical challenges in robotics. The natural structure of rigid body dynamics and the complementarity formulation of frictional impacts provide a framework for posing questions of stability and invariance as sums-of-squares optimization problems. This paper presents a class of algorithms for numerical computation of Lyapunov certificates for such systems. By invok-

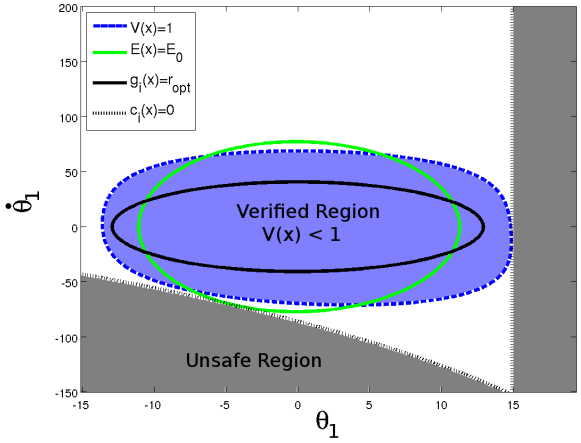

(a)

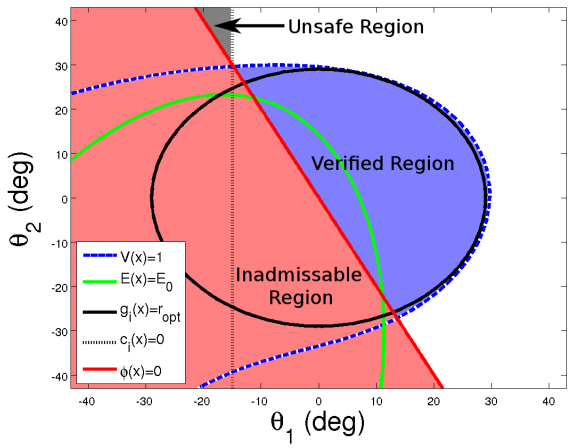

(b)

Figure 4: (a) A slice of the glider state space where the tail is restricted to the surface of the wall. The shaded blue region within the dashed line indicates the verified region $\mathcal{C} \cap \mathcal{A}$ for a quartic Lyapunov function and the solid black ellipse outlines $\mathcal{G}_i$. The green ellipse indicates the maximal sublevel set of energy that does not intersect the unsafe region, shown in gray. (b) A second slice of state space where the joint velocities are zero is also shown. In this slice, the general quartic Lyapunov function vastly outperforms energy and $\mathcal{G}_i$ is tight to $\mathcal{C}$.

ing the complementarity model of contact, we avoid directly reasoning about both the complexity of Zeno phenomena and the combinatorial number of hybrid modes associated with the set of potential contact states. Initial experiments have found physically significant certificates of stability and invariance for multiple problems of interest to the robotics community.

In this work, we have been primarily interested in stability in the sense of Lyapunov and positive invariance, but we hope to extend these methods to asymptotic stability. Here, we briefly discuss some of the challenges posed by this extension. Two common approaches to verifying asymptotic stability are to find a Lyapunov candidate where $\dot{V}$ is strictly negative or to apply LaSalle's Invariance Principle. With the former method, energy no longer provides an initial feasible candidate to begin bilinear alternation. In [12], Theorem 6.31 gives a generalization of LaSalle to discontinuous systems with the additional condition that the limit sets of trajectories also be positively invariant. The algorithms presented here might be extended to meet this condition and search for certificates of asymptotic stability.

Future work in this area will also center on extending these algorithms to more complex tasks. In particular, we are interested in the analysis of trajectories and limit cycles of robotics systems, where previous work has demonstrated the effectiveness of SOS based methods [19]. Numerical Lyapunov analysis has also been experimentally demonstrated to be an effective tool for controller synthesis, both at fixed points and along trajectories [18]. Furthermore, a natural extension of this work would be to include elastic impacts, where many models exist which are amenable to complementarity formulations such as in [28]. Recent work on the computation of regions of attraction for polynomial systems has included methods for approximating the volume of semialgebraic sets [11]. A similar approach here might eliminate the requirement for bilinear alternations and allow the problem to be posted as a single convex optimization program.

7. ACKNOWLEDGMENTS

This work was supported by the National Science Foundation [Contract IIS-1161679] and Defense Advanced Research Projects Agency program [BAA-10-65-M3-FP-024].

APPENDIX

A. PROOFS

The following proof is for Lemma 2.

PROOF. Fix a solution $x(t) = (q(t), v(t))$ with $x^-(t_0) \in \mathcal{C}$. Let $\bar{\tau}$ be the supremum over all τ such that $x^-(t) \in \mathcal{C}$ for all $t \in [t_0, \tau]$. Assume for contradiction $\bar{\tau}$ is finite. We see $x^-(\bar{\tau}) \in \mathcal{C}$ as it is the limit of a sequence in a connected component. The function $s \mapsto (q(\bar{\tau}), \bar{v}(s))$ is a path from $x^-(\bar{\tau})$ to $x^+(\bar{\tau})$. This path lies in Ω_c as $\mathrm{d}V \leq 0$ on $\mathcal{C}$ implies $V(x^-(\bar{\tau})) \leq V(x^-(t_0)) < c$ and, by assumption, $V(q(\bar{\tau}), \bar{v}(s))$ is a non-increasing function of s. The path lies in $\mathcal{A}$ as only the generalized velocities vary (recall our definition of $\mathcal{A}$ in (3)). Thus $x^+(\bar{\tau})$ belongs to $\mathcal{C}$. As $V(x^+(\bar{\tau})) < c$ and V is continuous, there exists an $r > 0$ such that:

$$U_r = \{x \in \mathbb{R}^{2n} \mid \|x - x^+(\bar{\tau})\|_\infty < r\}$$

is contained in Ω_c (where $\|\cdot\|_\infty$ is the maximum norm). As $x^+(\tau)$ is a right limit there exists an $\epsilon > 0$ such that $x(t) \in U_r$ for $t \in (\bar{\tau}, \bar{\tau} + \epsilon)$.

We show that $x(t) \in \mathcal{C}$ for almost all $t \in (\bar{\tau}, \bar{\tau} + \epsilon)$, contradicting the definition of $\bar{\tau}$. Fix t such that $v(t)$ is defined and examine the following functions:

$$\sigma_1 \mapsto (q(\sigma_1), v^+(\bar{\tau})),$$
$$\sigma_2 \mapsto (q(t), \sigma_2 v(t) + (1 - \sigma_2) v^+(\bar{\tau})),$$

the first defined for $\sigma_1 \in [\bar{\tau}, t]$ and the second for $\sigma_2 \in [0, 1]$. The second function is clearly continuous, and the first is continuous as $q(t)$ is continuous. We see the range of both maps lie in $\mathcal{A}$ as $\{q(t)\} \times \mathbb{R}^n \subset \mathcal{A}$ for all $t \geq t_0$. We see the ranges of the functions also lie in U_r: the first lies in U_r as $(q_1, v_1), (q_2, v_2) \in U_r$ implies $(q_2, v_1) \in U_r$ and the second as U_r is convex. Together these functions provide a path from $x^+(\bar{\tau})$ to $x(t)$ that lies in $\Omega_c \cap \mathcal{A}$, thus $x(t) \in \mathcal{C}$. □

The following proof is for Lemma 3.

PROOF. That (ii) implies (i) is the content of Lemma 2. Now assume (i) holds and fix a solution $(q(t), v(t))$ with $(q(t), v^-(t)) \in \mathcal{C}$. For convenience, let q,v^+, and v^- denote $q(t), v^+(t), v^-(t)$. Take the path $\bar{v}(s) = sv^+ + (1 - s)v^-$. Since V is convex in v and $\mathrm{d}V \leq 0$, we know

$$V(q, v^-) \geq (1 - s)V(q, v^-) + sV(q, v^+) \geq V(q, \bar{v}(s)),$$

so that the chord $(q, \bar{v}(s))$ lies in Ω_c, and clearly lies in $\mathcal{A}$.

We show that $\frac{dV(q,\bar{v}(s))}{ds} \leq 0$. Observe that $\{(q, \bar{v}(s) | s \in [0, 1)\}$ are all possible pre-impact states since $\phi(q) = 0$ and the impact conditions $Jv^- < 0, Jv^+ = 0$ imply that $J\bar{v}(s) < 0$. Let Λ_N be a feasible impulse such that $v^+ = v^- + H^{-1}J^T\Lambda_N$. Substituting into the definition of $\bar{v}(s)$,

$$\bar{v}(s) = v^- + sH^{-1}J^T\Lambda_N.$$

Since the constraints on Λ_N are linear, we know that the impulse $(1 - s)\Lambda_N > 0$ will also be feasible. Applying this impulse to $(q, \bar{v}(s))$ we get the post-impact velocity

$$\bar{v}^+(s) = \bar{v}(s) + (1 - s)H^{-1}J^T\Lambda_N = v^+.$$

And so v^+ is a possible post-impact velocity from an impact at any point along the chord. Since $\mathrm{d}V \leq 0$, we then know $V(q, \bar{v}(s)) \geq V(q, v^+)$. This implies that the minimum of V along the chord is achieved at (q, v^+) and, since V is convex, the derivative along the chord must be non-positive. □

B. BILINEAR ALTERNATION

Sum-of-squares optimization enables optimization over linearly parameterized polynomials that are guaranteed to be non-negative. This can be extended to guarantee non-negativity on basic semialgebraic sets in the following fashion[23]. To demonstrate that $g(x) \geq 0$ implies $f(x) \geq 0$ we introduce multiplier polynomials $\sigma_i(x)$ and require:

$$\sigma_1(x)f(x) - \sigma_2(x)g(x) \geq 0, \quad \sigma_1(x) - 1 \geq 0, \quad \sigma_2(x) \geq 0.$$

In general, we may wish to simultaneously search over the free coefficients of the multiplier polynomials $\sigma_i(x)$ and those of $f(x)$ and $g(x)$. However, such coefficients enter the condition in a bilinear fashion. Fixing the free coefficients of f and g, we can search over the free coefficients of σ_1 and σ_2, and vice versa. These allows for a coordinate-descent strategy where each step consists of a single convex optimization problem and is guaranteed to improve the objective value. Similar approaches have been applied to determine region-of-attraction estimates for smooth dynamical systems [32].

C. REFERENCES

[1] R. Alur, T. Henzinger, G. Lafferriere, and G. Pappas. Discrete abstractions of hybrid systems. *Proceedings of the IEEE*, 88(7):971 –984, july 2000.

[2] V. Bhatt and J. Koechling. Three-dimensional frictional rigid-body impact. *Journal of applied mechanics*, 62:893, 1995.

[3] M. Branicky, V. Borkar, and S. Mitter. A unified framework for hybrid control: model and optimal control theory. *Automatic Control, IEEE Transactions on*, 43(1):31 –45, jan 1998.

[4] B. Brogliato. *Nonsmooth mechanics: models, dynamics, and control*. Springer Verlag, 1999.

[5] A. Chatterjee and A. Ruina. A new algebraic rigid-body collision law based on impulse space considerations. *Journal of Applied Mechanics*, 65(4):939–951, 1998.

[6] M. J. Coleman, A. Chatterjee, and A. Ruina. Motions of a rimless spoked wheel: a simple 3d system with impacts. *Dynamics and Stability of Systems*, 12(3):139–160, 1997.

[7] S. H. Collins, A. Ruina, R. Tedrake, and M. Wisse. Efficient bipedal robots based on passive-dynamic walkers. *Science*, 307:1082–1085, February 18 2005.

[8] A. L. Desbiens, A. Asbeck, and M. Cutkosky. Hybrid aerial and scansorial robotics. *ICRA*, May 2010.

[9] E. L. Glassman, A. L. Desbiens, M. Tobenkin, M. Cutkosky, and R. Tedrake. Region of attraction estimation for a perching aircraft: A Lyapunov method exploiting barrier certificates. In *Proceedings of the 2012 IEEE International Conference on Robotics and Automation (ICRA)*, 2012.

[10] D. Henrion and A. Garulli, editors. *Positive Polynomials in Control*. Lecture Notes in Control and Information Sciences. Springer-Verlag, 2005.

[11] D. Henrion, J. Lasserre, and C. Savorgnan. Approximate volume and integration for basic semialgebraic sets. *SIAM Review*, 51(4):722–743, 2009.

[12] R. Leine and N. van de Wouw. *Stability and convergence of mechanical systems with unilateral constraints*. Springer Verlag, 2008.

[13] R. Leine and N. van de Wouw. Stability properties of equilibrium sets of non-linear mechanical systems with dry friction and impact. *Nonlinear Dynamics*, 51(4):551–583, 2008.

[14] R. Lind, G. Balas, and A. Packard. Evaluating D-K iteration for control design. In *American Control Conference, 1994*, volume 3, pages 2792 – 2797 vol.3, june-1 july 1994.

[15] J. Löfberg. YALMIP : A toolbox for modeling and optimization in MATLAB. In *Proceedings of the CACSD Conference*, Taipei, Taiwan, 2004.

[16] J. Lofberg. Pre- and post-processing sum-of-squares programs in practice. *IEEE Transactions On Automatic Control*, 54(5):1007–, May 2009.

[17] J. Lygeros, K. Johansson, S. Simic, J. Zhang, and S. Sastry. Dynamical properties of hybrid automata. *Automatic Control, IEEE Transactions on*, 48(1):2 – 17, jan 2003.

[18] A. Majumdar, A. A. Ahmadi, and R. Tedrake. Control design along trajectories with sums of squares programming. *Under review*, 2013.

[19] I. R. Manchester. Transverse dynamics and regions of stability for nonlinear hybrid limit cycles. *Proceedings of the 18th IFAC World Congress, extended version available online: arXiv:1010.2241 [math.OC]*, Aug-Sep 2011.

[20] A. Megretski. Systems polynomial optimization tools (SPOT), available online: `http://web.mit.edu/ameg/www/`. 2010.

[21] Y. Or and A. Ames. Stability and completion of zeno equilibria in lagrangian hybrid systems. *Automatic Control, IEEE Transactions on*, 56(6):1322 –1336, june 2011.

[22] A. Papachristodoulou and S. Prajna. Robust stability analysis of nonlinear hybrid systems. *Automatic Control, IEEE Transactions on*, 54(5):1035 –1041, may 2009.

[23] P. A. Parrilo. Semidefinite programming relaxations for semialgebraic problems. *Mathematical Programming*, 96(2):293–320, 2003.

[24] S. Prajna and A. Rantzer. Convex programs for temporal verification of nonlinear dynamical systems. *SIAM Journal of Control and Optimization*, 46(3):999–1021, 2007.

[25] E. Routh. *Dynamics of a system of rigid bodies*. MacMillan and co. London, 1891.

[26] A. S. Shiriaev and L. B. Freidovich. Transverse linearization for impulsive mechanical systems with one passive link. *IEEE Transactions On Automatic Control*, 54(12):2882–2888, December 2009.

[27] D. Stewart. Rigid-body dynamics with friction and impact. *SIAM Review*, 42(1):3–39, 2000.

[28] W. Stronge. Rigid body collisions with friction. *Proceedings of the Royal Society of London. Series A: Mathematical and Physical Sciences*, 431(1881):169–181, 1990.

[29] J. F. Sturm. Using SeDuMi 1.02, a Matlab toolbox for optimization over symmetric cones. *Optimization Methods and Software*, 11(1-4):625 – 653, 1999.

[30] R. Tedrake, I. R. Manchester, M. M. Tobenkin, and J. W. Roberts. LQR-Trees: Feedback motion planning via sums of squares verification. *International Journal of Robotics Research*, 29:1038–1052, July 2010.

[31] C. Tomlin, I. Mitchell, A. Bayen, and M. Oishi. Computational techniques for the verification of hybrid systems. *Proceedings of the IEEE*, 91(7):986 – 1001, july 2003.

[32] U. Topcu, A. Packard, and P. Seiler. Local stability analysis using simulations and sum-of-squares programming. *Automatica*, 44(10):2669 – 2675, 2008.

[33] C. W. Wampler and A. J. Sommese. Numerical algebraic geometry and algebraic kinematics. *Acta Numerica*, 20:469–567, 2011.

[34] Y. Wang and M. T. Mason. Two-dimensional rigid-body collisions with friction. *ASME Journal of Applied Mechanics*, 59:635–642, 1992.

[35] E. R. Westervelt, J. W. Grizzle, C. Chevallereau, J. H. Choi, and B. Morris. *Feedback Control of Dynamic Bipedal Robot Locomotion*. CRC Press, Boca Raton, FL, 2007.